Separation of Co(II)/Ni(II) with Cyanex 272 using a flat membrane microcontactor : extraction kinetics study

Separation of Co(II)/Ni(II) with Cyanex 272 using a flat membrane microcontactor: extraction kinetics study

Jonas Hereijgers[a,c], Tobias Vandermeersch[a], Nicolas Van Oeteren[a], Harry Verelst[a], Huiying Song[b], Deirdre Cabooter[b], Tom Breugelmans[c] and Wim De Malsche[a*]

[a]*Department of Chemical Engineering, Vrije Universiteit Brussel, Pleinlaan 2, 1050 Brussel, Belgium*

[b]*Department for Pharmaceutical and Pharmacological Sciences, Pharmaceutical Analysis, KU Leuven – University of Leuven, Herestraat 49, 3000 Leuven, Belgium*

[c]*Faculty of Applied Engineering, Research group Advanced Reactor Technology, University of Antwerp, Salesianenlaan 90, 2660 Hoboken, Belgium*

*Corresponding author: tel. (+) 32/ 2.629.33.18, fax (+) 32/ 2.629.32.48, e-mail:

wdemalsc@vub.ac.be

Abstract

In the present study, the extraction kinetics of cobalt with Cyanex 272 in a flat membrane microcontactor is studied. Pseudo-first order and non-first order models are proposed to describe the extraction kinetics with acidic Cyanex 272 and saponified Cyanex 272. The impact of the buffer concentration, the Cyanex 272 concentration, the feed concentration, the channel depth and saponification of Cyanex 272 was experimentally measured on the extraction kinetics. From this, it was shown that for acidic Cyanex 272 pseudo-first order reaction kinetics could be assumed under at least following conditions: (1) when the feed was buffered; (2) the Cyanex 272 concentration was 4.4 times higher than the cobalt concentration ; and (3) the cobalt concentration remained below 0.0167 mol/L. In that case a linear model could be derived that could be solved analytically. At higher cobalt concentrations saturation of the interface had to be taken into account, resulting in a non-linear model that had to be solved numerically. When Cyanex 272 was saponified the extraction kinetics dropped significantly indicating that pseudo-first order kinetics does not apply any longer. Hence, faster extraction kinetics in membrane contactors with acidic Cyanex 272 is obtained by buffering the feed phase compared to the saponification approach of Cyanex 272.

Keywords

solvent extraction; membrane contactor; cobalt; saponified Cyanex 272; microreactor

List of Symbols

r	reaction rate	[mol/(m³ s)]
k_r	reaction rate constant	$[(m^3)^{0.67}/(mol^{0.67}\ s)]$
k'_r	reaction rate constant independent of the interfacial area	$[(m^3)^{0.67}/(mol^{0.67}\ s\ m^2)]$
C	concentration	[mol/L]
J	flux	[mol/(m² s)]
k	local mass transfer coefficient	[m/s]
K_M	global mass transfer coefficient	[m/s]
Sh	Sherwood number	[/]
D	diffusion coefficient	[m²/s]

F	flow rate	[m³/s]
d	diameter	[m]
r	radius	[m]
R	coil radius	[m]
h	channel depth	[m]
u	velocity	[m/s]
x	axial position inside the MMC	[m]
X	distance	[m]
t	time	[s]
L	length of the MMC	[m]
Δx	spatial step size	[m]
K_{eq}	equilibrium constant	[/]
K_{ad}	adsorption constant (ratio of the adsorption rate over desorption rate)	[/]

Greek symbols

$\mu_{1,t}$	first central time moment	[s]
$\mu'_{2,t}$	second central time moment	[s²]
η	dynamic Viscosity	[Pa.s]
ρ	density	[kg/m³]
ε	porosity of the membrane	[\]
τ	tortuosity of the membrane	[\]
δ	thickness of the membrane	[m]

Subscript

Co^{2+}	aqueous cobalt
Na-DDPA	saponified di- decylphosphinic acid
$CoR_2(HR)_2$	cobalt-Cyanex 272 complex
$(HR)_2$	acidic Cyanex 272
H^+	proton
R^-	saponified Cyanex 272
R	raffinate
E	extract
t	tube
trans	transition
m	membrane
eff	effective
b	bulk
x	axial position inside the MMC
i	interface
eq	equilibrium
in	inlet
LDF	linear driving force model
ad	adsorption
*	free sites

1 Introduction

Cobalt and nickel are among the most important non-ferrous metals and consequently their separation is a key process in hydrometallurgy [1], [2]. Typical hydrometallurgical separation processes like chemical precipitation and oxidation are however not economically feasible due to the similar physicochemical properties of cobalt and nickel. Fortunately, solvent extraction (SX) of cobalt easily allows the separation of cobalt from nickel. It is estimated that in the western hemisphere 40% of cobalt is produced using SX with bis(2,4,4-trimethylpentyl)phosphinic acid (Cyanex 272) as the extraction solvent [3]. Traditionally, SX is performed in packed columns, centrifugal extractors or mixer-settler tanks. Although these systems have been the workhorses for decades now, important problems such as foaming, flooding, unloading, the need for a density difference and stable emulsion formation still present important disadvantages [4], [5]. The use of membrane contactors offers a route to avoid these problems, as the phases are contacted in a non-dispersive manner [6], [7]. Hence, as long as the pressure difference across the membrane remains beneath a critical pressure, the breakthrough pressure, the interface between both liquids remains fixed at the pore mouth by capillary action [8] and both phases are contacted in a non-dispersive manner. Above this breakthrough pressure, the non-wetting phase will displace the wetting liquid inside the pores and disperse at the opposite side of the membrane into this wetting phase. This should be avoided at all times.

Two different operating modes exist for membrane contactors: batch mode [9], [10] and continuous flow mode [11], [12]. Membrane contactors in batch consist of two chambers separated by a membrane that allows extraction of cobalt by diffusion through the membrane. The advantage of this approach is the possibility to insert an agitator at each side of the membrane and mix each chamber separately, intensifying mass transfer. While this configuration can be utilized for lab-scale experiments it cannot be scaled up for industrial use [13]. To allow a scaling-up, flow membrane contactors are required, as they have more favorable mass transfer characteristics. These devices can either be semi-continuous or fully continuous. Semi-continuous contactors consist of a closed system

wherein the feed and solvent are continuously recycled, while passing several times through the membrane contactor. In a fully continuous system the feed and solvent only pass the membrane contactor once, allowing an easier downstream processing (e.g. extractant regeneration).

The membrane used in a flow configuration can either be of a flat sheet [6] or a hollow fiber configuration [4]. The hollow fiber approach has as disadvantage that a bundle of fibers can result in shell side by-passing, due to the presence of channeling paths in between fibers (shell side). Secondly, for sealing a potting adhesive is used to separate the lumen side of the fibers from the shell side. This potting adhesive however is prone to attacks by the organic solvent. The advantage of the hollow fibers is that they are self-supporting and have typically inner diameters of 200-300 µm and walls of a few tens of micrometers thick [4], resulting in a large specific surface ranging from 500-5000 m^2/m^3 [14]. The flat sheet configuration on the other hand requires a support, which is typically 0.5 to 10 mm thick [15], as a result the specific surface in such flat sheet membrane contactors is only 100-2000 m^2/m^3. As for typical operation conditions flows are laminar inside such flat sheet membrane contactors, mass transfer is purely diffusion based, leading to slow extraction kinetics.

With current microfabrication technology [16] it is possible to fabricate structured supports with depths of hundred micrometer and less, creating a specific surface larger than 10000 m^2/m^3. Such membrane microcontactors (MMC) allow to reach equilibrium within just a few minutes [6].

A special application of membrane contactors is supported liquid membrane extraction (SLM). In SLM the pores of the membrane are filled with organic extractant, such that at both sides of the membrane the aqueous feed and stripping phase can be used, requiring only one membrane unit for extraction and stripping [10], [12]. However, long-term stability poses a considerable problem [17], [18]. Unavoidably, extractant will be gradually lost in one of the aqueous phases by either dissolution or drag forces. Consequently, if there is no renewal strategy (e.g. dispersed extractant in the stripping phase) [19] both aqueous phases will eventually come into contact, undoing the separation partially or completely.

The separation of cobalt with Cyanex 272 in a flow MMC has already been studied by some authors [11], [19], [20]. Soldenhoff et al. [11] specifically studied a fully continuous one pass membrane contactor device and reported an overall mass transfer coefficient in the order of 10^{-7} m/s. However, looking at non-reactive extraction cases [7] and other hydrometallurgical [21]–[23] SX cases using membrane contactors, the overall mass transfer coefficient is expected to be an order of magnitude larger. To explain this, Soldenhoff et al. used the resistances-in-series model to describe the global mass transfer coefficient and added an additional term: the reaction rate resistance. By fitting, they claimed that this difference, that was as large as an order of magnitude, is primarily caused by the slow reaction kinetics. However, using a Lewis cell, a global mass transfer coefficient of several orders of magnitude larger was reported [24] due to vigorously mixing, reducing mass transfer resistance. If indeed the reaction rate would be limiting this would not be possible and the global mass transfer coefficient obtained with the Lewis cell should still be in the same order of magnitude as the one reported by Soldenhoff et al. Xing et al. [25] also experimentally determined the reaction rate (Eq.1) for saponified di-decylphosphinic acid (Na-DDPA), which is very similar to saponified Cyanex 272, as it only differs in its aliphatic chains (see Fig. A.1):

$$-r_{Co^{2+}} = k_r * C_{Co^{2+}}^{0.96} * C_{Na-DDPA}^{0.71} \quad (1)$$

with r the reaction rate, k_r the reaction rate constant dependent of the interfacial area, C the concentration. Consequently, it can be assumed that the reaction rate constant (Eq. 2, [25]) with Cyanex 272 is at least of the same order of magnitude as the one reported by Xing et al. [25], which is still several orders of magnitude larger than the local mass transfer coefficients:

$$k_r = 4.48 * 10^{-6} \frac{(m^3)^{0.67}}{mol^{0.67} s} \; (A_{interface} = 21.19\ cm^2) \quad (2a)$$

$$k'_r = 2.11 * 10^{-3} \frac{(m^3)^{0.67}}{mol^{0.67} s\ m^2_{interface\ area}} \quad (2b)$$

with k'_r the reaction rate constant independent of the interfacial area. Hence, in membrane contactors the mass transfer towards the extraction solvent is purely diffusion based and because of it a few orders of magnitude lower than the reaction rate. Therefore the extraction kinetics is only mass transfer limited. Soldenhoff et al. also used the resistances-in-series model to describe the global mass transfer coefficient. However, the resistances are only additive when the reaction kinetics are first order or pseudo-first order [26].

In this work, the extraction of cobalt with Cyanex 272 is studied. The selectivity, influence of buffer, Cyanex 272 and feed concentration, channel depth and saponification of Cyanex 272 on the overall extraction kinetics are studied and a model is proposed to describe the observed results.

2 Material and methods

2.1 Chemicals

Cyanex 272 (45 wt% in escaid 110, 1.260 mol/L) from Cytec (NJ, US) was used without further purification. Acetic acid, sodium hydroxide, n-heptane, cobalt(II)sulfate heptahydrate and nickel(II)sulfate hexahydrate were delivered by Sigma-Aldrich (Belgium) with a purity of 99+%. Calibration solutions of 1000 mg/ml Co^{2+} and Ni^{2+} for the atomic absorption spectroscopic analysis were purchased from Chem-Lab (Belgium). The water used throughout the experiments was prepared in the laboratory (Milli-Q-gradient, Millipore, MA, USA).

2.2 Construction of the MMC

The MMC (Fig. 1) consisted of two polyoxymethylene (POM) bodies. A tri-layered polypropylene/polyethylene/polypropylene membrane (Celgard 2320, d_{pore} = 27 nm, thickness = 20 µm, porosity = 39 %) was clamped between these two bodies in which a channel was milled, containing diamond shaped pillars to support the membrane (Datron M7 CNC mill). At the inlet these diamond shaped pillars had an aspect ratio (AR) (length/width) of 10, allowing the incoming liquid to

be uniformly distributed over the entire width of the channel. Subsequently, wedges were used to pass these pillars of AR 10 over into pillars of AR 1 (Fig. 1a) to increase the internal volume. The spacing between the pillars was 300 µm throughout the entire channel. The channel was 13 mm wide, 99 mm long and 50 or 100 µm deep, resulting in an internal volume of 37 or 74 µl. Before clamping, the membrane was stretched around the POM body to avoid rippling and a Kalrez o-ring (Eriks, Belgium) was placed around the channel to ensure sealing upon clamping. An aluminum holder was placed around the POM bodies and tightened with bolts in stages from 1 Nm to 2.5 Nm, 5 Nm and finally 7.5 Nm using a torque wrench to guarantee a uniform clamping strength of the POM bodies.

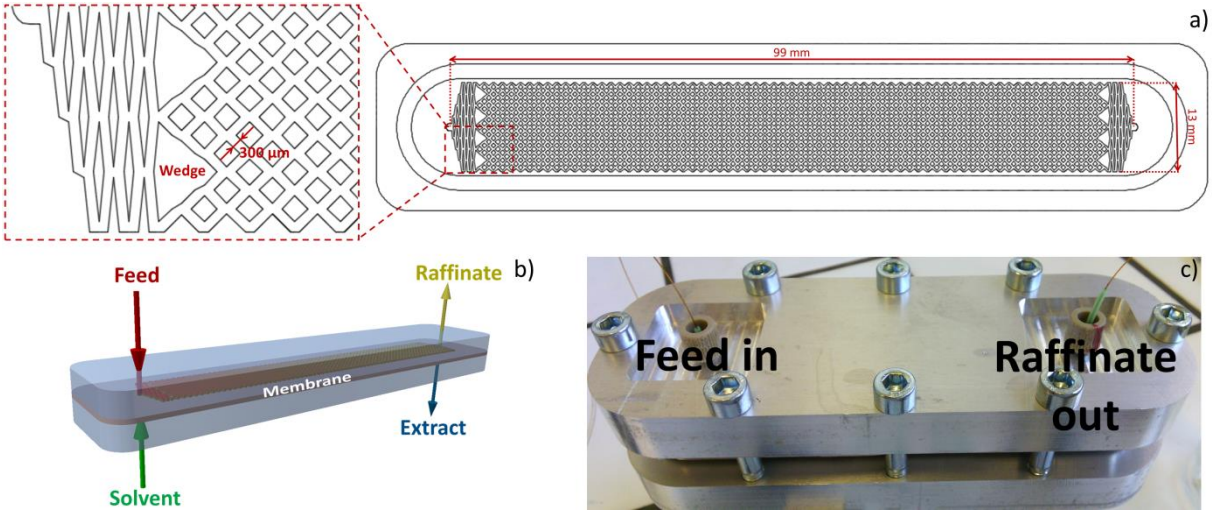

Fig. 1: a) Top view representation of the MMC channel, b) 3D representation of the MMC and c) picture of the fully assembled MMC.

2.3 Extraction experiments

The feed was freshly prepared to avoid salting out by dissolving cobalt(II)sulfate heptahydrate and nickel(II)sulfate hexahydrate in water. In case that an acetate buffer was used, acetic acid was added and the pH was adjusted to the desired value using 10.0 mol/L NaOH and a glass electrode (WTW Inolab). The solvent consisted of Cyanex 272 in escaid 110 (1.260 mol/L) and was further diluted in n-heptane when required. In case saponified Cyanex 272 was used, NaOH was added to saponify 60% of the Cyanex 272 and stirred until a homogeneous phase was obtained. The feed solution and

extraction solvent were fed into the MMC at a flow rate ratio of 1:1 at different flow rates using two HPLC pumps (Shimadzu, LC10AD) and capillaries with an internal diameter of 200 µm as a connection. After flushing the internal volume of the entire system three times, a steady-state condition was assumed and samples of the raffinate were collected at the outlet in an ice bath. These samples were subsequently diluted with 0.4 mol/L hydrochloric acid solution and analyzed using atomic absorption spectroscopy (ICE 3000 AA Spectrometer Thermo Scientific). From these results the amount extracted was calculated using Eq. 3:

$$\%\, Extracted = \frac{C_{Feed} - C_{Raffinate}}{C_{Feed}} * 100 \quad (3)$$

Every sample was visually controlled for phase homogeneity to ensure a breakthrough-free operation. Before starting a new extraction campaign, a start-up procedure was performed to avoid the presence of air bubbles. The start-up procedure consisted of flushing the MMC set-up with isopropanol for 5 min at a flow rate of 5 ml/min. By doing so, all air inside the MMC channel and inside the pores of the membrane is removed, as by capillary action isopropanol is drawn into the pores. Subsequently, the feed and organic solvent (n-heptane with Cyanex 272) is pumped into the MMC for 5 min to replace all isopropanol inside the MMC channels and membrane.
Batch tests were performed to determine the equilibrium. 5 ml of feed was mixed with 5 ml of organic solvent and shaken manually for 5 min. Both phases were separated by gravitation settling. Once separated a sample was taken from the raffinate phase and analyzed.

2.4 Measurement of the diffusion coefficient

The bulk diffusion coefficient (D_{bulk}) of acidic Cyanex 272 was measured at a constant temperature of 22.5°C in pure heptane using the Taylor-Aris procedure [27]. A plug of acidic Cyanex 272 was injected in a capillary with a length L = 15.24 m and an inner diameter d_t = 0.051709 cm, coiled to a radius R = 12 cm at a flow rate of 0.10 mL/min. Under these conditions axial diffusion can be ignored and the

width of the peak will be controlled by the radial diffusion of acidic Cyanex 272 in the capillary against the parabolic flow profile, according to:

$$\mu'_{2,t} = \frac{d_t^2 \mu_{1,t}}{96 D_{bulk}} \quad (4)$$

This allows calculating D_{bulk} from the first ($\mu_{1,t}$) and second central ($\mu'_{2,t}$) time moments of the recorded peak profiles (Eq. 4). The injected volume was 1 µL. Effects of secondary flow could be ignored since the applied flow rate was lower than the transition flow rate F_{trans} (Eq. 5):

$$F_{trans} = \sqrt{\frac{518 R r_t D_{bulk} \eta}{\rho}} \quad (5)$$

with r_t the radius of the capillary, η the viscosity and ρ the density of the solvent. Under the conditions applied here, F_{trans} was 0.13 mL/min, hence satisfying the condition of $F < F_{trans}$.

All experiments were performed on a Perkin Elmer 275 UHPLC system (Perkin Elmer, Waltham, MA, USA) equipped with a binary high-pressure gradient pump, a cooled auto-sampler and a variable wavelength detector with a flow cell of 2.6 µL. The dwell volume of the system was 600 µL and the maximum operating pressure was 700 bar (10,000 psi). Chromera software was used for system operation and data evaluation (Perkin Elmer).

3 Results

3.1 Extraction kinetics model

The extraction of cobalt with Cyanex 272 is an equilibrium reaction in which protons are exchanged for cobalt ions. Hence, control of the pH is crucial to shift the equilibrium and two different methods can be used for this purpose. In the first method, the pH of the aqueous feed phase is regulated (e.g. by buffering or continuously adding NaOH) and proceeds by following overall reaction (Eq. 6) [9], [12], [28], [29]:

$$Co_{aq}^{2+} + 2(HR)_{2,org} \rightleftharpoons CoR_2.(HR)_{2,org} + 2H^+ \quad (6)$$

In the second method Cyanex 272 is partially saponified (Eq. 7) before contacting it with the aqueous cobalt feed. The overall reaction (Eq. 8) [10], [30], [31] therefore differs from Eq. 6:

$$2NaOH_{aq} + (HR)_{2,org} \rightleftharpoons 2NaR_{org} + 2H_2O_{aq} \quad (7)$$

$$Co^{2+}_{aq} + R^{-}_{org} + 2(HR)_{2,org} \rightleftharpoons CoR_2.3HR_{org} + H^{+}_{aq} \quad (8)$$

Next to the two Cyanex 272 dimer complexes an additional sapponified Cyanex 272 molecule takes part in the reaction. Consequently, the model with acidic Cyanex 272 and the partially saponified Cyanex 272 will be inherently different. See the appendix (§A.2) for the derivation of the different models.

Due to the difference in the equilibrium constant (Eqs. A.3 and A.19) a slight difference appears in the final equations (Eqs. A.13 and A.21) for the pseudo-first order models of acidic and saponified Cyanex 272. However, this difference is marginal as can be seen in Fig. 2 when using the parameters in Table 1. In Table 1 the diffusion coefficients were taken from literature or determined with the method given in §2.4 (see Table 3), K_{eq} for acidic Cyanex 272 was determined by fitting (see §3.2.3) and K_{eq} for saponified Cyanex 272 was determined from a batch test (see §3.2.6). Hence, when pseudo-first order is assumed no difference is expected in the extraction kinetics between acidic Cyanex 272 and saponified Cyanex 272.

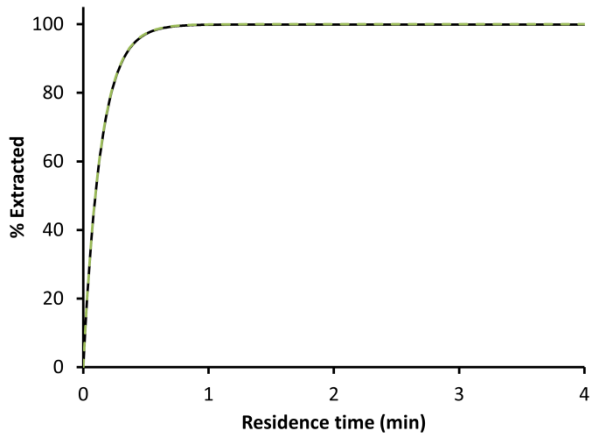

Fig. 2: The solid black line represents the acidic Cyanex 272 pseudo-first order model. The green dotted line represents the saponified Cyanex 272 pseudo-first order model. The models were calculated using the parameters in Table 1.

Table 1: Parameters used for deriving the pseudo-first order models in Fig. 2.

	Acidic Cyanex 272	***60% Saponified Cyanex 272***
h	*50 µm*	*50 µm*
$C_{Co^{2+},R,in}$	*0.0142 mol/L*	*0.0142 mol/L*
$C_{(HR)_2,E,in}$	*0.630 mol/L*	*0.252 mol/L*
$C_{R^-,E,in}$	/	*0.756 mol/L*
$C_{H^+,R,in}$	10^{-7} *mol/L*	10^{-7} *mol/L*
$D_{bulk,Co^{2+},R}$	6.4×10^{-10} *m²/s*	6.4×10^{-10} *m²/s*
$D_{bulk,CoR_2.(HR)_2,E}$	2.506×10^{-10} *m²/s*	2.506×10^{-10} *m²/s*
K_{eq}	3.27×10^{-11}	2.83×10^{-7}

When the concentration Cyanex 272 can no longer be assumed constant no longer pseudo-first order kinetics can be assumed and the non-first order models apply. Looking at Fig. 3, there is a distinct difference in extraction kinetics between the acidic Cyanex 272 and the saponified Cyanex 272. To calculate the non-first order model for saponified Cyanex 272, it was assumed that the diffusion coefficients are the same as in acidic Cyanex 272 (Table 2). The diffusion coefficients were taken from literature or determined with the method given in §2.4 (see Table 3). For saponified Cyanex 272 the same diffusion coefficient was taken as for acidic Cyanex 272, as it was not found in the literature and cannot be determined with the method given in §2.4. Hence, with 60 % saponified Cyanex 272 there is also acidic Cyanex 272 present inside the solution, preventing the determination of the diffusion coefficient of solely saponified Cyanex 272, as 100 % saponified Cyanex 272 solidifies. K_{eq} for acidic Cyanex 272 was determined by fitting (see §3.2.3) and K_{eq} for saponified Cyanex 272 was determined from a batch test (see §3.2.6). However, since the viscosity increases with saponified Cyanex 272 [24], it is likely that the diffusion coefficients are even lower in the organic phase,

increasing the difference between the acidic Cyanex 272 and saponified Cyanex 272 non-first order model even more.

This slower extraction rate is not what is expected, since the extraction with saponified Cyanex 272 is reported to occur faster than with acidic Cyanex 272 [24]. However, Fu et al. [24] used a Lewis Cell that mixed the organic and aqueous phase active without disrupting the interface, hence strongly lowering mass transfer resistance, making reaction kinetics again relevant.

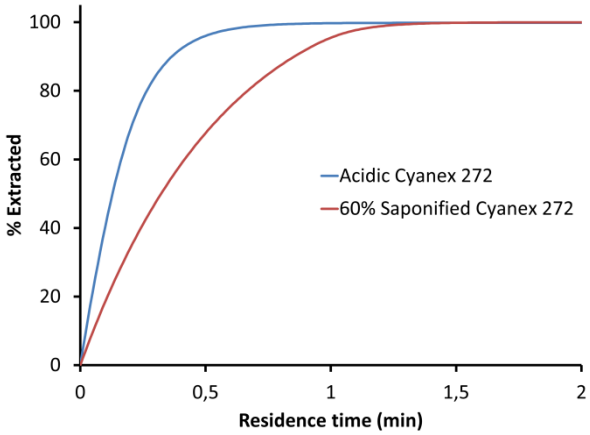

Fig. 3: The blue line represents the acidic Cyanex 272 non-first order model. The red line represents the saponified Cyanex 272 non first order model. The models were calculated using the parameters in Table 2.

Table 2: Parameters used for deriving the non-first order models in Fig. 3.

	Acidic Cyanex 272	***60% Saponified Cyanex 272***
h	*50 µm*	*50 µm*
$C_{Co^{2+},R,in}$	*0.1067 mol/L*	*0.1067 mol/L*
$C_{(HR)_2,E,in}$	*0.630 mol/L*	*0.252 mol/L*
$C_{R^-,E,in}$	*/*	*0.756 mol/L*
$C_{H^+,R,in}$	*10^{-7} mol/L*	*10^{-7} mol/L*
$D_{bulk,Co^{2+},R}$	*6.4 x 10^{-10} m²/s*	*6.4 x 10^{-10} m²/s*
$D_{bulk,(HR)_2,E}$	*4.842 x 10^{-10} m²/s*	*4.842 x 10^{-10} m²/s*
$D_{bulk,R^-,E}$	*/*	*4.842 x 10^{-10} m²/s*
$D_{bulk,CoR_2.(HR)_2,E}$	*2.506 x 10^{-10} m²/s*	*2.506 x 10^{-10} m²/s*
K_{eq}	*3.27 x 10^{-11}*	*2.83 x 10^{-7}*

To check the validity of all these proposed models they are compared against experimental results in the following section. This allows to identify which of the made assumptions were correct.

3.2 Experimental validation

3.2.1 Selectivity

As the pH strongly influences the amount extracted and the selectivity, it was kept constant during extraction by adding an acetate buffer. The acetate buffer was assumed not to take part in the complex formation process as is reported for similar extractants (D_2EHPA, LIX 860-I and Cyanex 301) [32]. As the amount extracted in function of the pH strongly depends on the operating conditions and was not reported in literature when an acetate buffer is added, this was determined using shake tests (Fig. 4a and Fig. A.5). The pH-isotherm was also represented in function of the pH of the feed before extraction instead of the equilibrium pH, as inside the MMC pH-regulation was not possible.

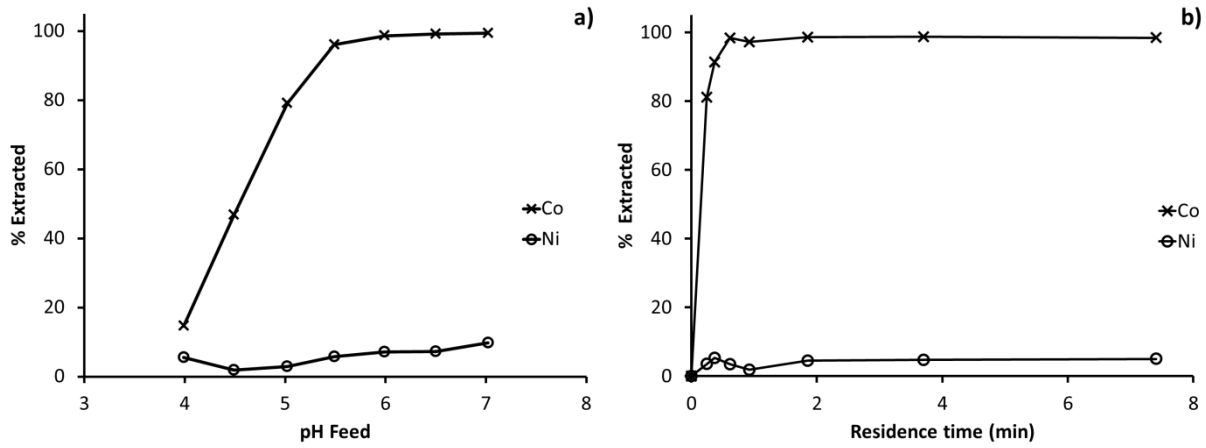

Fig. 4: a) pH isotherm for 0.0142 mol/L $CoSO_4$ and 0.0038 mol/L $NiSO_4$ with 0.5 mol/L acetate buffer and 0.252 mol/L acidic Cyanex 272. The pH in the x-axis denotes the pH of the feed solution before extraction. b) Extraction performance for the MMC with h = 50 µm, Celgard 2320 membrane, 0.0142 mol/L $CoSO_4$, 0.0038 mol/L $NiSO_4$, 0.5 mol/L acetate buffer pH = 7 and 0.252 mol/L acidic Cyanex 272.

At pH 7 99.4% of the cobalt was extracted. Consequently, all the following MMC experiments were conducted at pH 7. At higher pH values more nickel was co-extracted and cobalt precipitated. When pH dropped during extraction, there was a certain margin as at pH 6 still 98.6% of the cobalt was extracted. In Fig. 4b the extraction performance was plotted for the MMC. At 0.6 min equilibrium was reached and 98.3% of the cobalt was extracted, whereas only 4% of the nickel was extracted.

3.2.2 Influence of acetate buffer concentration

To derive the models it was assumed that the concentration of H^+ remained constant as the aqueous phase was buffered. Looking at Fig. 5 this was justified. With a concentration of 0.0142 mol/L Co^{2+} and 1.260 mol/L acidic Cyanex 272 and a channel depth of 50 µm there was no difference in the measured extraction kinetics of cobalt (data points) for the buffer concentrations: 0.5, 1.0 and 2.0 mol/L (pH = 7). Non-diluted (1.260 mol/L) acidic Cyanex 272 was used as it was expected that the impact of the buffer concentration on the extraction kinetics would be most pronounced. Hence, with a higher concentration acidic Cyanex 272 the viscosity is larger, potentially decreasing the

extraction kinetics. If this would be the case, the impact due to the buffer concentration would be more visible. However, both the concentration buffer as the concentration acidic Cyanex 272 (see § 3.2.3) did not influence the extraction kinetics.

In order to evaluate the acidic Cyanex 272 pseudo-first order and the non-first order model, the diffusion coefficients of $CoSO_4$ and Co-Cyanex 272 complex were taken from literature (see Table 3) and for acidic Cyanex 272 a diffusion coefficient of 4.842×10^{-10} m²/s in n-heptane was determined with the method given in §2.4 (Fig. A.6). The equilibrium constant of 3.27×10^{-11} was determined from the MMC experiments at different acidic Cyanex 272 concentrations (see further). Using these data, the extraction kinetics could be predicted without a further need for any experimental extraction measurements in the MMC. Hence, looking at Fig. 5 the two models (black solid line and red dotted line) gave the same result, which coincided well with the experimental data points. For the acidic Cyanex 272 pseudo-first order model the global mass transfer coefficient amounted to 5.97×10^{-6} m/s, in line with other non-reactive extraction [7] and hydrometallurgical SX [21]–[23]cases. The small difference between the experimental data and the theoretical models could be due to deviations of the Sherwood number (0.94 ± 0.17) or of the reported diffusion coefficients. For instance, if the acidic Cyanex 272 pseudo-first order model was fitted using the data points by varying the diffusion coefficient of $CoSO_4$ in water, the sum of least squared errors was the smallest at a diffusion coefficient of 2.90×10^{-10} m²/s, which was close to the diffusion coefficient used from literature (Table 3). However, for a further validation of the proposed models the diffusion coefficients reported in the literature were used. As there was no difference between the different buffer concentrations, a 0.5 mol/L acetate buffer was used for the rest of the experiments.

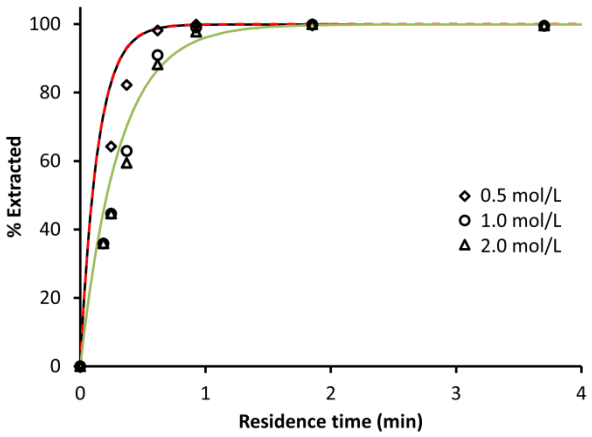

Fig. 5: Impact of the acetate buffer concentration (pH = 7) onto the extraction kinetics of cobalt, under the following conditions: 1.260 mol/L acidic Cyanex 272, 0.0142 mol/L $CoSO_4$, h = 50 µm, Celgard 2320 membrane. The points represent experimental measurements. The black solid line represents the acidic Cyanex 272 pseudo-first order model and the red dotted line the acidic Cyanex 272 non-first order model. The green solid line represents the fitted acidic Cyanex 272 pseudo-first order model.

Table 3: The molecular diffusion coefficient of CoSO4 (aqueous), acidic Cyanex 272 (n-heptane) and Co-Cyanex 272 (kerosene).

Compound (solvent)	Diffusion coefficient	Reference
$CoSO_4$ (aqueous)	6.4 x 10^{-10} m²/s	[33]
Acidic Cyanex 272 (n-heptane)	4.842 x 10^{-10} m²/s	§2.4
Co-Cyanex 272 (kerosene[a])	2,506 x 10^{-10} m²/s	[9]

[a] Slight deviation with the diffusion coefficient in n-heptane could exist. However, the impact of the diffusion coefficient of Co-Cyanex 272 on the models is negligible.

3.2.3 Influence of Cyanex 272 concentration

From Fig. 5 it was clear that at 1.260 mol/L Cyanex 272 concentration and 0.0142 mol/L $CoSO_4$ there was no difference between the pseudo-first order and the non-first order acidic Cyanex 272 model. It is therefore justified to assume that the Cyanex 272 concentration was constant with concomitant pseudo-first order kinetics. This was also checked for lower concentrations of Cyanex 272 (Fig. 6). By fitting the equilibrium constant, a value of K_{eq} = 3.27 x 10^{-11} was obtained and from 1.260 mol/L to

0.063 mol/L Cyanex 272 with 0.0142 mol/L $CoSO_4$ the extraction kinetics coincided well with the experimental data for the acidic Cyanex 272 pseudo-first order model. Hence, it was valid to assume that the Cyanex 272 concentration remained constant, for the studied ratio range of acidic Cyanex 272 concentration over $CoSO_4$ concentration going from 88.7 to 4.4. At lower ratios it could very well be that the concentration of acidic Cyanex 272 can still be assumed constant, but this has not been investigated as at these lower ratios the amount of cobalt extracted is low and thus of limited interest.

Because the concentration of acidic Cyanex 272 can indeed be assumed constant, the model remains linear and analytically solvable. With 0.063, 0.126 and 0.252 mol/L Cyanex 272 respectively 69.4%, 93.8% and 98.7% of the cobalt was extracted. From Fig. 6 it could be seen that with 0.0142 mol/L $CoSO_4$ higher Cyanex 272 concentrations than 0.252 mol/L yielded roughly the same extraction performance.

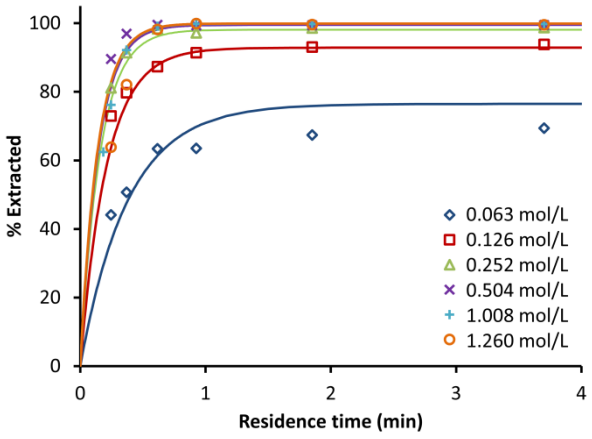

Fig. 6: Impact of the acidic Cyanex 272 concentration onto the extraction kinetics of cobalt under following conditions: 0.5 mol/L acetate buffer pH = 7, 0.0142 mol/L $CoSO_4$, h = 50 µm, Celgard 2320 membrane. The solid lines represent the acidic Cyanex 272 pseudo-first order model.

3.2.4 Influence of Co^{2+} concentration

To derive the proposed models above, it was also assumed that the interfacial surface was not saturated. When the cobalt concentration in the feed was increased, the flux should also increase

linearly (Eq. A.8), not affecting the extraction kinetics. With SLM experiments however Swain et al. [10] reported that the flux reaches a plateau at a cobalt concentration of 0.0114 mol/L with 0.750 mol/L Cyanex 272. For a Cyanex 272 concentration of 1.260 mol/L in Fig. 7 a similar effect was observed. An acidic Cyanex 272 concentration of 1.260 mol/L was chosen to keep the percentage cobalt extracted constant (~100%), allowing to study the impact of the cobalt concentration, as the concentration acidic Cyanex 272 does not influence the extraction kinetics (see §3.2.3). In Fig. 7 it is seen that at the cobalt concentration of 0.0167 mol/L, the data points are still satisfactorily described by the acidic Cyanex 272 pseudo-first order model (black dotted line), which neglects interface saturation. However, at cobalt concentrations of 0.0579 mol/L and 0.1125 mol/L it was no longer valid to neglect interface saturation. Hence, saturation at the interface had to be taken into account and consequently the equilibrium constant (Eq. A.3) had to be rewritten to Eq. 9:

$$K_{eq} = \frac{C_{CoR_2.(HR)_2,m,i,x}\ C_{H^+,R,in}^2\ C_*}{C_{Co^{2+},R,ad,x}\ C_{(HR)_2,E,in}^2} \tag{9}$$

with C_* the concentration of free sites and $C_{Co^{2+},R,ad,x}$ the concentration of cobalt adsorbed at the interface at position x. To describe the concentration of cobalt adsorbed at the interface, the linear driving force (LDF) model (Eq.10) proposed by Glueckauf [34], which also equaled Eq. A.17, was used:

$$J_{Co^{2+},ad} = k_{LDF}\left(C_{Co^{2+},R,ad,eq,x} - C_{Co^{2+},R,ad,x}\right) \tag{10}$$

with k_{LDF} the effective LDF mass transfer coefficient and $C_{Co^{2+},R,ad,eq,x}$ the adsorbed concentration of cobalt when equilibrium would be reached. $C_{Co^{2+},R,ad,eq,x}$ could be calculated using the Langmuir adsorption isotherm (Eq. A.11):

$$C_{Co^{2+},R,ad,eq,x} = \frac{K_{ad}\ C_{Co^{2+},R,i,x}\ C_*}{1 + K_{ad}\ C_{Co^{2+},R,i,x}} \tag{11}$$

with K_{ad} the ratio of the adsorption rate over the desorption rate. Combining Eqs. A.2, A.4 and A.5 with Eqs. 9-11 gave a non-linear system such as in the non-first order models and had to be solved numerically in a similar fashion (Eq. A.53).

By the sum of least squared errors, this adapted model was fitted to the experimental data points to determine the concentration of free sites, K_{ad} and k_{LDF} (Table 4) which is represented in Fig. 7 by the solid colored lines. By adding the LDF model in combination with the Langmuir adsorption isotherm, the model now did take saturation of the interface into account. At residence times yielding higher extraction efficiencies than 50 %, the model did not correspond as good to the experimental data as for shorter residence times for the two highest concentrations. This might be attributed to a decreased molecular diffusion at increasing concentrations. It might also be related to a deviation of Langmuir adsorptive behavior at increasing concentrations. Further work is required to investigate this rigorously. As K_{ad} is large, one could simplify the Langmuir adsorption isotherm into Eq. 12:

$$C_{Co^{2+},R,ad,eq,x} = C_* \tag{12}$$

Doing so the function describing $C_{Co^{2+},R,i,x}$ reduces from a third order polynomial (Eq. A.53) to a second order polynomial (Eq. A.58), simplifying the numerical calculations. However, then a different curve was obtained (Fig. 7 colored dotted line) as at a certain position x in the MMC the concentration $C_{Co^{2+},R,i,x}$ becomes so low that the denominator in Eq. 11 can no longer be simplified, prohibiting the made simplification (Eq. 12).

Table 4: The fitted values for the concentration free sites, K_{ad} and k_{LDF}.

C_*	5.147 x 10^{-7} mol/L
K_{ad}	5.5 x 10^{15}
k_{LDF}	0.065 m/s

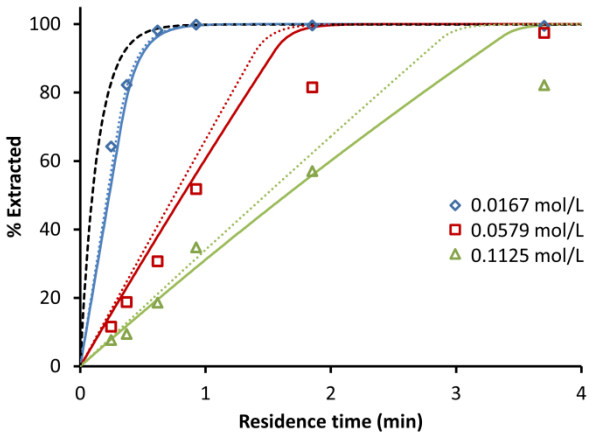

Fig. 7: Impact of the feed concentration of $CoSO_4$ onto the extraction kinetics of cobalt under following conditions: 0.5 mol/L acetate buffer pH = 7, 1.260 mol/L Cyanex 272, h = 50 µm, Celgard 2320 membrane. The solid colored lines represent the model containing the Langmuir LDF model. The colored dotted lines represent the model containing the LDF model with the simplified Langmuir adsorption isotherm (Eq. 12). The black dotted line represent the acidic Cyanex 272 pseudo-first order model, neglecting saturation of the interface.

3.2.5 Influence of the channel depth

From Eq. A.9 it is clear that the channel depth strongly influences the extraction kinetics. However, as decreasing the channel depth had a positive impact on the extraction kinetics (Fig. 8a) it also reduced the internal volume of the MMC from 74 µl to 37 µl, if the channel depth was lowered from 100 µm to 50 µm. Despite this lower internal volume the throughput in terms of flow rate increased (Fig. 8b). This can be understood from the fact that the transport from the raffinate to the extract solely depends upon diffusion and in that case the time (t) needed to diffuse a certain distance (X) is related to that distance with the power of 2 (Eq. 13), whereas the internal volume scales linearly with the channel depth.

$$X^2 = 2Dt \tag{13}$$

Therefore, a decrease in channel depth has a positive impact on throughput, despite a decrease of the internal volume and residence time (Fig. 8b). However, one should remark that with decreasing

channel depth the pressure drop increases, eventually leading to breakthrough. For both channel depths the acidic Cyanex 272 pseudo-first order model coincided with the experimental data points.

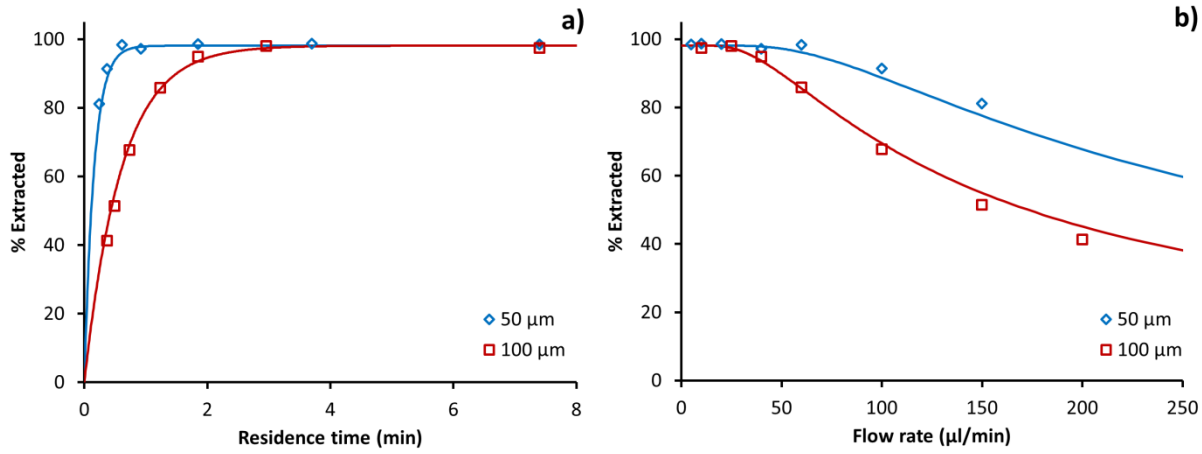

Fig. 8: Impact of the channel depth onto the extraction kinectis of cobalt in function of a) residence time and b) flow rate, under following conditions: 0.5 mol/L acetate buffer pH 7, 0.0142 mol/L $CoSO_4$, 0.252 mol/L Cyanex 272, Celgard 2320 membrane. The solid lines represent the acidic Cyanex 272 pseudo-first order model.

3.2.6 Influence of saponification

When Cyanex 272 was saponified, the extraction preceded much slower (Table 5). With 0.1067 mol/L Co^{2+} and 1.260 mol/L acidic Cyanex 272 (0.5 mol/L acetate buffer pH 7) 91.7 % of cobalt was extracted at a residence time of 14.8 min. However, with saponified Cyanex 272 at the same residence time only 39.8 % of the cobalt was extracted. Hence, to obtain fast extraction kinetics in membrane contactors buffering the feed is superior over saponification of Cyanex 272. Non-diluted (1.260 mol/L) Cyanex 272 was used as saponification of diluted Cyanex 272 gave rise to a third phase formation, because of its low solubility in n-heptane.

This difference in extraction kinetics was not caused by the lack of buffer with the saponified Cyanex 272 experiment, as when buffer was added the amount of cobalt that was extracted remained the same. This also justified the assumption of constant proton concentration that was made to derive the models for saponified Cyanex 272.

The slower extraction with saponified Cyanex 272 in the MMC could more likely be explained by the fact that pseudo-first order kinetics could not be assumed for saponified Cyanex 272. Consequently, also diffusion of the Cyanex 272 should be taken into account as it indeed slowed down the extraction kinetics (Fig. 3). This also explained the results reported by Soldenhoff et al. [11]. Here Cyanex 272 was also saponified, and Soldenhoff et al. found a global mass transfer coefficient in the range of 4.3 - 7.3 x 10^{-7} m/s with a fiber radius of 120 µm, whereas for the acidic Cyanex 272 experiments with a channel depth of 50 and 100 µm (Fig. 7) the global mass transfer coefficient was respectively 2.8 x10^{-6} m/s and 5.5 x10^{-6} m/s. Hence, the reaction kinetics is indeed to be neglected as it otherwise would also had to be seen in the experiments with acidic Cyanex 272, which has an even slower reaction kinetics than with saponified Cyanex 272 [24].

One could also try to explain these observed results by the fact that the viscosity of the organic phase increases with the amount of saponified Cyanex 272 [24], hence lowering the diffusion coefficients in the organic phase. Saponified Cyanex 272 is reported to polymerize [29], which increases the viscosity. If however a pseudo-first order kinetics is then still assumed, the diffusion coefficient of the cobalt-Cyanex 272 complex would have to drop with 5-6 orders of magnitude to comply with the observed results. This is so because the global mass transfer coefficient (Eq. A.9) for extraction mainly depends on the first term. However, such a value of a diffusion coefficient is considered to be very unlikely, even when taking the polymerization effect into account. However, when non-first order kinetics was assumed, the diffusion coefficients in the organic phase had a much large impact on the extraction kinetics (Fig. 9). In Fig. 9 the impact of the diffusion coefficients in the organic phase on the amount of cobalt extracted is depicted, which was calculated using the non-first order model for a fixed residence time of 0.5 min. Using the diffusion coefficients from Table 3 59.4 % of cobalt should be extracted according to the non-first order model, which does not comply with the observed results (Table 5). However, when the diffusion coefficients in the organic phase only dropped with a factor of 16, the model does describe the observed results (Table 5) correctly. This decrease of the diffusion coefficients, due to the polymerization effect, seems more plausible then

with the pseudo-first order model, were the diffusion coefficient of the Co-Cyanex 272 complex had to drop with 5-6 orders of magnitude to describe the observed results satisfactory. As K_{eq} was defined differently for saponified Cyanex 272 (Eq. A.19), it was determined from a batch test and equaled to 2,83 $x10^{-7}$.

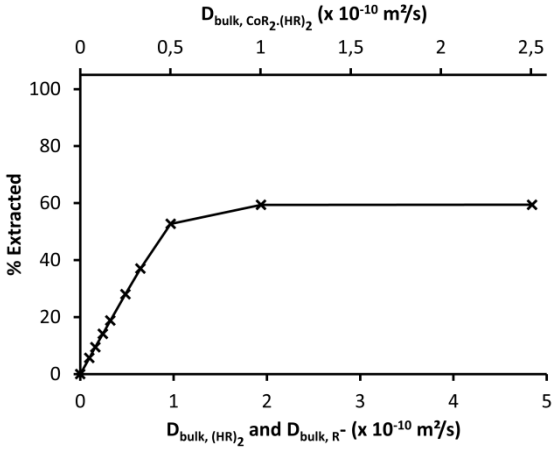

Fig. 9: Numerical simulation of the impact of the diffusion coefficient of acidic Cyanex 272, saponified Cyanex 272 and loaded Cyanex 272 on the extraction kinetics for the non-first order saponified Cyanex 272 model under following conditions: $t_{residence}$ = 0.5 min, h = 100 µm, 0.0142 mol/L $CoSO_4$, 1.260 mol/L Cyanex 272 of which 60 procent was saponified, Celgard 2320 membrane, K_{eq} = 2.83 x 10^{-7}.

Table 5: The amount of cobalt extracted in a MMC (h = 100 µm, Celgard 2320) with 1.260 mol/L acidic Cyanex 272 (acetate buffer 0.5 mol/L pH = 7) or 60% saponified Cyanex 272 with and without 0.5 mol/L acetate buffer (pH = 7).

Concentration Co^{2+}	Residence time	Acidic Cyanex 272	Saponified Cyanex 272	Saponified Cyanex 272 + Acetate buffer
0.0142 mol/L	0.5 min	63.8 %	17.6%	/
0.0534 mol/L	3.7 min	90.5%	32.7%	/
0.1067 mol/L	14.8 min	91.7%	39.8%	38.4%

4 Conclusions

To describe the extraction kinetics for cobalt with Cyanex 272 in a flat sheet membrane microcontactor, it was demonstrated that it was valid to assume pseudo-first order kinetics under at least the following studied conditions: (1) when the aqueous feed was buffered with an acetate buffer with a concentration in the range of 0.5 to 2.0 mol/L; (2) when the ratio of concentration acidic Cyanex 272 over concentration $CoSO_4$ was in the range of 88.7 to 4.4; and (3) when the concentration $CoSO_4$ was lower than 0.0167 mol/L. In this case the model remained linear and could be solved analytically. However, when the concentration of cobalt in the aqueous feed was higher than 0.0167 mol/L, saturation of the interface had to be taken into account. As a consequence, the model had to be solved numerically, however still agreeing with the experimental data.

When Cyanex 272 was saponified, a large decrease in extraction kinetics was observed in comparison with acidic Cyanex 272. This was not due to the reaction kinetics since it was not observed in the experiments with acidic Cyanex 272. It was more likely that pseudo-first order kinetics could not be assumed with saponified Cyanex 272. With the non-first order model for saponified Cyanex 272, a difference in extraction kinetics was observed and a small decrease in diffusion coefficient in the organic solvent due to an increase of viscosity could explain the slower extraction kinetics. Hence, to maximize extraction kinetics of cobalt with Cyanex 272 in membrane contactors, buffering of the feed is a superior approach over saponification of Cyanex 272.

5 Acknowledgements

W. De Malsche greatly acknowledges the Flemish Fund for Scientific Research (FWO) for support through a Post-Doctoral grant (81409). J. Hereijgers (111140) and T. Vandermeersch (110539) are supported through a specialization grant from the Instituut voor Wetenschap en Technologie (IWT) from the Flanders region.

The authors have declared no conflict of interest.

6. References

[1] E. Lindell, E. Jääskeläinen, E. Paatero, and B. Nyman, “Effect of reversed micelles in Co/Ni separation by Cyanex 272,” *Hydrometallurgy*, vol. 56, no. 3, pp. 337–357, 2000.

[2] J.-P. Yeh, R.-D. Chien, S.-C. Chen, and S.-H. Lin, “Extraction Separation of Co(II) from Ni(II) in H 2 SO 4 Solutions with Na-Cyanex 302 in Hollow-Fiber Contactors,” *Sep. Sci. Technol.*, vol. 48, no. 5, pp. 699–705, 2013.

[3] O. S. Ayanda, F. A. Adekola, A. A. Baba, B. J. Ximba, and O. S. Fatoki, “Application of Cyanex® extractant in Cobalt/Nickel separation process by solvent extraction,” *Int. J. Phys. Sci.*, vol. 8, no. 3, pp. 89–97, Jan. 2013.

[4] A. Gabelman and S. Hwang, “Hollow fiber membrane contactors,” *J. Memb. Sci.*, vol. 159, no. 1–2, pp. 61–106, Jul. 1999.

[5] J.-P. Yeh, S.-H. Lin, R.-D. Chien, S.-C. Chen, and H.-Y. Chiao, “Extraction separation of Co(II) from Ni(II) in H 2 SO 4 solutions with carriers in hollow-fiber contactors,” *Desalin. Water Treat.*, vol. 51, no. 25–27, pp. 5057–5063, 2013.

[6] J. Hereijgers, M. Callewaert, X. Lin, H. Verelst, T. Breugelmans, H. Ottevaere, G. Desmet, and W. De Malsche, “A high aspect ratio membrane reactor for liquid-liquid extraction,” *J. Memb. Sci.*, vol. 436, pp. 154–162, Feb. 2013.

[7] J. Hereijgers, N. van Oeteren, J. F. M. Denayer, T. Breugelmans, and W. De Malsche, “Multistage counter-current solvent extraction in a flat membrane microcontactor,” *Chem. Eng. J.*, vol. 273, pp. 138–146, 2015.

[8] J. Hereijgers, T. Breugelmans, and W. De Malsche, “Breakthrough in a flat channel membrane microcontactor,” *Chem. Eng. Res. Des.*, vol. 94, pp. 98–104, 2015.

[9] P. K. Parhi and K. Sarangi, “Separation of copper, zinc, cobalt and nickel ions by supported liquid membrane technique using LIX 84I, TOPS-99 and Cyanex 272,” *Sep. Purif. Technol.*, vol. 59, no. 2, pp. 169–174, 2008.

[10] B. Swain, J. Jeong, J. C. Lee, and G. H. Lee, “Extraction of Co(II) by supported liquid membrane and solvent extraction using Cyanex 272 as an extractant: A comparison study,” *J. Memb. Sci.*, vol. 288, no. 1–2, pp. 139–148, 2007.

[11] K. Soldenhoff, M. Shamieh, and A. Manis, “Liquid-liquid extraction of cobalt with hollow fiber contactor,” *J. Memb. Sci.*, vol. 252, no. 1–2, pp. 183–194, Apr. 2005.

[12] B. Swain, C. Mishra, J. Jeong, J. Lee, H. S. Hong, and B. D. Pandey, “Separation of Co(II) and Li(I) with Cyanex 272 using hollow fiber supported liquid membrane: A comparison with flat sheet supported liquid membrane and dispersive solvent extraction process,” *Chem. Eng. J.*, vol. 271, pp. 61–70, Jul. 2015.

[13] K. NATH, *Membrane Separation Processes*. PHI Learning Pvt. Ltd., 2008.

[14] M. Aguilar and J. L. Cortina, *Solvent Extraction and Liquid Membranes: Fundamentals and Applications in New Materials*. New York: CRC Press, 2008.

[15] Z. F. Cui and H. S. Muralidhara, *Membrane Technology - A Practical Guide to Membrane Technology and Applications in Food and Bioprocessing*. Elsevier Ltd, 2010.

[16] V. Hessel, A. Renken, J. C. Schouten, and J.-I. Yoshida, Eds., *Micro Process Engineering: A Comprehensive Handbook, Volume 1, 2&3*. Weinheim, Germany: Wiley-VCH Verlag GmbH & Co. KGaA, 2009.

[17] X. J. Yang, A. G. Fane, and K. Soldenhoff, "Comparison of Liquid Membrane Processes for Metal Separations: Permeability, Stability, and Selectivity," *Ind. Eng. Chem. Res.*, vol. 42, no. 2, pp. 392–403, Jan. 2003.

[18] P. K. Parhi, "Supported liquid membrane principle and its practices: A short review," *J. Chem.*, vol. 2013, 2013.

[19] Z. Ren, W. Zhang, H. Meng, J. Liu, and S. Wang, "Extraction separation of Cu(II) and Co(II) from sulfuric solutions by hollow fiber renewal liquid membrane," *J. Memb. Sci.*, vol. 365, no. 1–2, pp. 260–268, Dec. 2010.

[20] B. Swain, J. Jeong, J. C. Lee, and G. H. Lee, "Separation of Co(II) and Li(I) by supported liquid membrane using Cyanex 272 as mobile carrier," *J. Memb. Sci.*, vol. 297, no. 1–2, pp. 253–261, 2007.

[21] G. R. M. Breembroek, A. Van Straalen, G. J. Witkamp, and G. M. Van Rosmalen, "Extraction of cadmium and copper using hollow fiber supported liquid membranes," *J. Memb. Sci.*, vol. 146, no. 2, pp. 185–195, 1998.

[22] C. Yang and E. L. Cussler, "Reaction dependent extraction of copper and nickel using hollow fibers," *J. Memb. Sci.*, vol. 166, no. 2, pp. 229–238, 2000.

[23] K. Sarangi and R. P. Das, "Separation of copper and zinc by supported liquid membrane using TOPS-99 as mobile carrier," *Hydrometallurgy*, vol. 71, no. 3–4, pp. 335–342, Jan. 2004.

[24] X. Fu and J. A. Golding, "EQUILIBRIUM AND MASS TRANSFER FOR THE EXTRACTION OF COBALT AND NICKEL FROM SULFATE SOLUTIONS INTO BIS (2,4,4-TRIMETHYLPENTYL) PHOSPHINIC ACID - 'CYANEX 272'.," *Solvent Extr. Ion Exch.*, vol. 6, no. 5, pp. 889–917, Mar. 1988.

[25] P. XING, C. WANG, S. XU, and Z. JU, "Kinetics of cobalt(II) extraction from sulfate aqueous solution by sodium salt of di-decylphosphinic acid (DDPA)," *Trans. Nonferrous Met. Soc. China*, vol. 23, no. 2, pp. 517–523, 2013.

[26] E. L. Cussler, *Diffusion: Mass Transfer in Fluid Systems*, vol. Second. 1997.

[27] J. G. Atwood and J. Goldstein, "Measurements of diffusion coefficients in liquids at atmospheric and elevated pressure by the chromatographic broadening technique," *J. Phys. Chem.*, vol. 88, no. 9, pp. 1875–1885, Apr. 1984.

[28] B. K. Tait, “Cobalt-nickel separation: the extraction of cobalt(II) and nickel(II) by Cyanex 301, Cyanex 302 and Cyanex 272,” *Hydrometallurgy*, vol. 32, no. 3. pp. 365–372, Apr-1993.

[29] N. B. Devi, K. C. Nathsarma, and V. Chakravortty, “Sodium salts of D2EHPA, PC-88A and Cyanex-272 and their mixtures as extractants for cobalt(II),” *Hydrometallurgy*, vol. 34, no. 3, pp. 331–342, 1994.

[30] B. Swain, J. Jeong, J. Lee, and G. H. Lee, “Separation of cobalt and lithium from mixed sulphate solution using Na-Cyanex 272,” *Hydrometallurgy*, vol. 84, no. 3–4, pp. 130–138, Nov. 2006.

[31] K. Sarangi, B. R. Reddy, and R. P. Das, “Extraction studies of cobalt (II) and nickel (II) from chloride solutions using Na-Cyanex 272. Separation of Co(II)/Ni(II) by the sodium salts of D2EHPA, PC88A and Cyanex 272 and their mixtures,” *Hydrometallurgy*, vol. 52, no. 3, pp. 253–265, 1999.

[32] I. Van de Voorde, L. Pinoy, E. Courtijn, and F. Verpoort, “Influence of acetate ions and the role of the diluents on the extraction of copper (II), nickel (II), cobalt (II), magnesium (II) and iron (II, III) with different types of extractants,” *Hydrometallurgy*, vol. 78, no. 1–2, pp. 92–106, Jul. 2005.

[33] J. Xiong, P. M. May, and I. M. Ritchie, “The diffusion coefficient of cobalt(II) and bisulphate in moderately acidic sulphate solutions,” *Electrochimica Acta*, vol. 32, no. 7. pp. 1035–1038, Jul-1987.

[34] E. Glueckauf, “Theory of chromatography. Part 10. - Formulae for diffusion into spheres and their application to chromatography,” *Trans. Faraday Soc.*, vol. 51, p. 1540, Jan. 1955.